GeroScience (2024) 46:4615–4634
https://doi.org/10.1007/s11357-024-01172-6

ORIGINAL ARTICLE

Echocardiographic characterization of age- and sex-associated differences in cardiac function and morphometry in nonhuman primates

Maria Cristina Florio · Laura Fusini · Gloria Tamborini · Christopher Morrell · Alise McDonald · Michelle Walcott · Kenneth Ridley · Kelli L. Vaughan · Julie A. Mattison · Mauro Pepi · Edward G. Lakatta · Maurizio C. Capogrossi

Received: 16 February 2024 / Accepted: 21 April 2024 / Published online: 30 April 2024

Abstract Aging per se is a major risk factor for cardiovascular diseases and is associated with progressive changes in cardiac structure and function. Rodent models are commonly used to study cardiac aging, but do not closely mirror differences as they occur in humans. Therefore, we performed a 2D echocardiographic study in non-human primates (NHP) to establish age- and sex-associated differences in cardiac function and morphometry in this animal model. M mode and 2D echocardiography and Doppler analyses were performed cross-sectionally in 38 healthy rhesus monkeys (20 females and 18 males), both young (age 7–12 years; $n=20$) and old (age 19–30 years; $n=18$). The diameters of the cardiac chambers did not differ significantly by age group, but males had larger left ventricular diameters (2.43 vs 2.06 cm in diastole and 1.91 vs 1.49 cm in systole, $p=0.0004$ and $p=0.0001$, respectively) and left atrial diameter (1.981 vs 1.732 cm; $p=0.0101$). Left ventricular mass/body surface area did not vary significantly with age and sex. Ejection fraction did not differ by age and females presented a higher ejection fraction than males (54.0 vs 50.8%, $p=0.0237$). Diastolic function, defined by early to late mitral peak flow velocity ratio (E/A), was significantly lower in old rhesus monkeys (2.31 vs 1.43, $p=0.0020$) and was lower in females compared to males (1.595 vs 2.230, $p=0.0406$). Right ventricular function, evaluated by measuring the Tricuspid Annular Plane Systolic Excursion, did not differ by age or sex, and Right Ventricular Free Wall Longitudinal Strain, did not differ with age but was lower in males than in females (-22.21 vs -17.95%, $p=0.0059$). This is the first echocardiographic study to evaluate age- and sex-associated changes of cardiac morphometry and

Mauro Pepi, Edward G. Lakatta and Maurizio C. Capogrossi contributed equally to this work.

Supplementary Information The online version contains supplementary material available at https://doi.org/10.1007/s11357-024-01172-6.

M. C. Florio (✉) · C. Morrell · E. G. Lakatta · M. C. Capogrossi
Laboratory of Cardiovascular Science, Biomedical Research Center, Intramural Research Program, National Institute On Aging, NIH, Baltimore, MD, USA
e-mail: cristiflorio@gmail.com

L. Fusini · G. Tamborini · M. Pepi
Department of Cardiovascular Imaging, Centro Cardiologico Monzino - IRCCS, Milan, Italy

A. McDonald · M. Walcott · K. Ridley
Division of Cardiology, Johns Hopkins Bayview Medical Center, Baltimore, MD, USA

K. L. Vaughan · J. A. Mattison
Translational Gerontology Branch, National Institute on Aging, NIH Animal Center, Dickerson, MD, USA

M. C. Capogrossi (✉)
Division of Cardiology, The Johns Hopkins University School of Medicine, Baltimore, MD, USA
e-mail: mcapogr1@jhmi.edu

function in young and old NHP. The findings of this work will provide a reference to examine the effect of age and sex on cardiac diseases in NHP.

Keywords Aging · Diastolic function · Heart failure · Monkeys · Nonhuman primates

Introduction

The number of older people living in developed countries has progressively increased and it is now estimated that about 20% of the world's population will be older than 65 years by 2050 [1]. Consequently, the effect of aging on the heart and blood vessels leading to left ventricular diastolic and systolic dysfunction and, ultimately, to heart failure (HF), has global impact. Heart failure with preserved ejection fraction (HFpEF) is the predominant form of HF in advanced age affecting 59% of all patients older than 85 years [2], and is the main cause of morbidity, hospitalization, and mortality in subjects above 65 years of age [3]. Moreover, HFpEF is more prevalent in females compared to males with a ratio of 4:1 [4, 5], and temporal trends show that the prevalence of HFpEF relative to HF with reduced ejection fraction (HFrEF) increases at a rate of 1% per year, after 50 years of age [5–8].

The mechanisms underlying the age- and sex-association of heart disease in humans are still largely unknown and most translational studies in this area have been performed in mice and rats. Although rodents are a tremendously valuable model for biomedical research, they do not always mimic the clinical picture or pathophysiology seen in humans. Therefore, a NHP model that most closely mirrors human physiology and pathology is more likely to yield clinically relevant results compared to rodents [9]. Due to their similarities to humans, rhesus macaques (*Macaca mulatta*) are the most frequently used NHP in biomedical research. In rhesus monkeys, the rate of aging is approximately three times that of humans, although this ratio is not exactly constant throughout every stage of life [10, 11].

Many cardiovascular diseases (CVDs) can be identified and diagnosed via echocardiography, a non-invasive and commonly used approach, and the echocardiographic characterization for NHP in the context of cardiovascular research is incomplete. Previous echocardiographic studies have evaluated either small cohorts of NHP with very limited age ranges [12–16] or with allometric scaling of echocardiographic parameters to body weight [17].

The objectives of this project are to evaluate age- and sex-associated differences in systolic and diastolic function, as well as cardiac structure, via M and 2D echocardiography, in healthy rhesus monkeys without evidence of any other CV pathologic condition. This study provides an analysis and comparison of echocardiographic reference values among young and elderly, male and female NHP and addresses similarities and differences between rhesus monkeys and humans.

Material and methods

Non-human primates

The study population of 38 adult rhesus monkeys (20 females and 18 males) aged 7 to 30 years were grouped as young (9.3 ± 1.1 years, $n = 10$ females and 10 males) or old (22.4 ± 2.7 years, $n = 10$ females and 8 males) (Table 1). These monkeys in captivity previously reported a median survival of approximately 26 years of age and 10% survival of 35 years of age [11, 18, 19]. All NHP were evaluated for the presence of pathologic conditions that could influence cardiac function including a detailed blood chemistry profile (Supplementary Table S1); one rhesus monkey was removed from the study because diabetic.

NHP were maintained at the NIH Animal Center (Poolesville, MD) and housed in standard primate caging with a controlled temperature (25.5 ± 0.5° C) and humidity (60 ± 20%) and a 12-h light–dark cycle. Commercially prepared monkey chow (Lab Diet #5038, Lab-Diet Inc., St. Louis, MO) was distributed twice daily, supplemented with daily food enrichment, and water was available ad libitum. All procedures were conducted in accordance with the Guide for the Care and Use of

Table 1 Demographics: mean (±SD) age in years by experimental group

	Young	Old
Female	8.9 (±1.0)	22.6 (±1.9)
	$n = 10$	$n = 10$
Male	9.7 (±0.9)	22.1 (±3.3)
	$n = 10$	$n = 8$

Laboratory Animals and approved by the NIA Intramural Research Program's Animal Care and Use Committee.

Cardiovascular exams were performed while rhesus monkeys were anesthetized following an overnight fast. All NHP were sedated using Ketamine (5 mg/kg, IM) and Dexmedetomidine (0.02 mg/kg, IM), with Atipamezole reversal (0.2 mg/kg, IV and/or IM), as needed. Heart rate, systolic and diastolic blood pressure, oxygen saturation, and rectal body temperature were monitored continuously throughout each procedure via a BM7 Vet Pro patient monitoring system (Bionet America, Inc., Tustin, CA). Measurements of height (crown-rump length) were made between the cranial vertex and the apex of the sacrum using a standard measuring tape.

Body surface area (BSA) was calculated using the Dubois formula modified for rhesus where crown to rump is measured, as previously described [20]. All echocardiographic examinations were performed with an Acuson S2000® ultrasound system (Siemens, Mountain View, CA). A complete standard M-mode and two-dimensional echocardiography was performed with the rhesus monkeys in dorsal recumbency, slightly tilted towards the left lateral decubitus position. All NHP tolerated anaesthesia well and no complications were reported during the procedure or following completion of the study. In all NHP, the echocardiographic exam yielded acquisitions of excellent quality.

Echocardiographic measurements

M-mode parameters were measured from the parasternal long axis view, according to American Society of Echocardiography (ASE) guidelines [21]: left atrial diameter (LAd), left ventricular (LV) outflow diameter (LVOTd), diastolic interventricular septum (IVS), LV posterior wall (LVPW) thickness, relative wall thickness, and end diastolic and systolic LV diameters (LVEDd and LVESd, respectively). Figure 1 shows an example of 2D images of the heart.

LV fractional shortening (LVFS) was calculated as

$$LVFS(\%) = \left[\frac{LVDd - LVDs}{LVDd}\right]x100\%$$

LV end diastolic (LVEDV) and end systolic (LVESV) volumes were calculated with the corrected Teichholz formula: $LVEDV = \frac{7xLVEDd^3}{2.4+LVEDd}$ and $LVESV = \frac{7xLVESd^3}{2.4+LVESd}$, respectively.

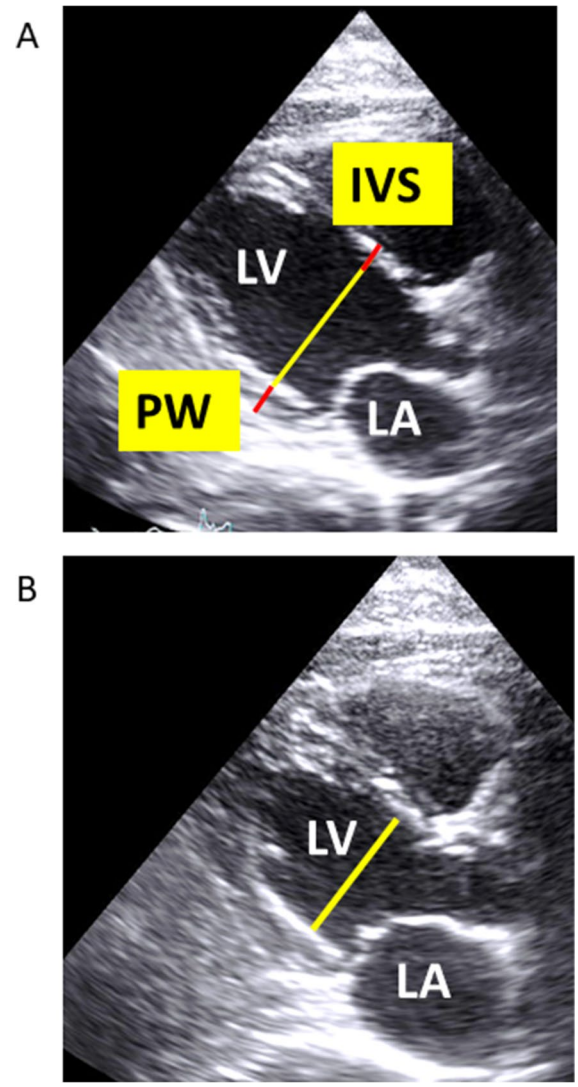

Fig. 1 Representative 2D TTE images of the parasternal long axis view of the heart. **A** Diastolic and **B** Systolic frames. Examples of measurements of the diastolic and systolic diameters of the left ventricle (LV) and of the interventricular septal (IVS) and posterior wall (PW) thickness. (LA: left atrium)

LV ejection fraction was calculated according to

$$LVEF(\%) = \left[\frac{LVEDV - LVESV}{LVEDV}\right]x100\%$$

LV mass (LVM) was obtained as [22]

$$LVM(g) = 0.8x1.04x\left[(IVS + LVEDd + PWT)^3 - LVEDd^3\right] + 0.6g$$

Relative wall thickness was obtained as

$$RWT = IVS + LVPW/LVEDd$$

Figure 2 provides examples of relevant functional parameters by 2D TTE, M mode, and Doppler.

Pulsed-wave Doppler was performed to measure LV outflow velocity–time integral (LVOvti) in 5 chamber view while LVOT area (LVOTa) was derived from LVOT diameter (LVOTd):

$$LVOTa = \pi(\frac{LVOTd}{2})^2$$

Peak systolic velocity and velocity time integral (AOvti) of aortic systolic flow were measured from 5 chamber apical view. Aorta valve area (AVA) was calculated with continuity equation as

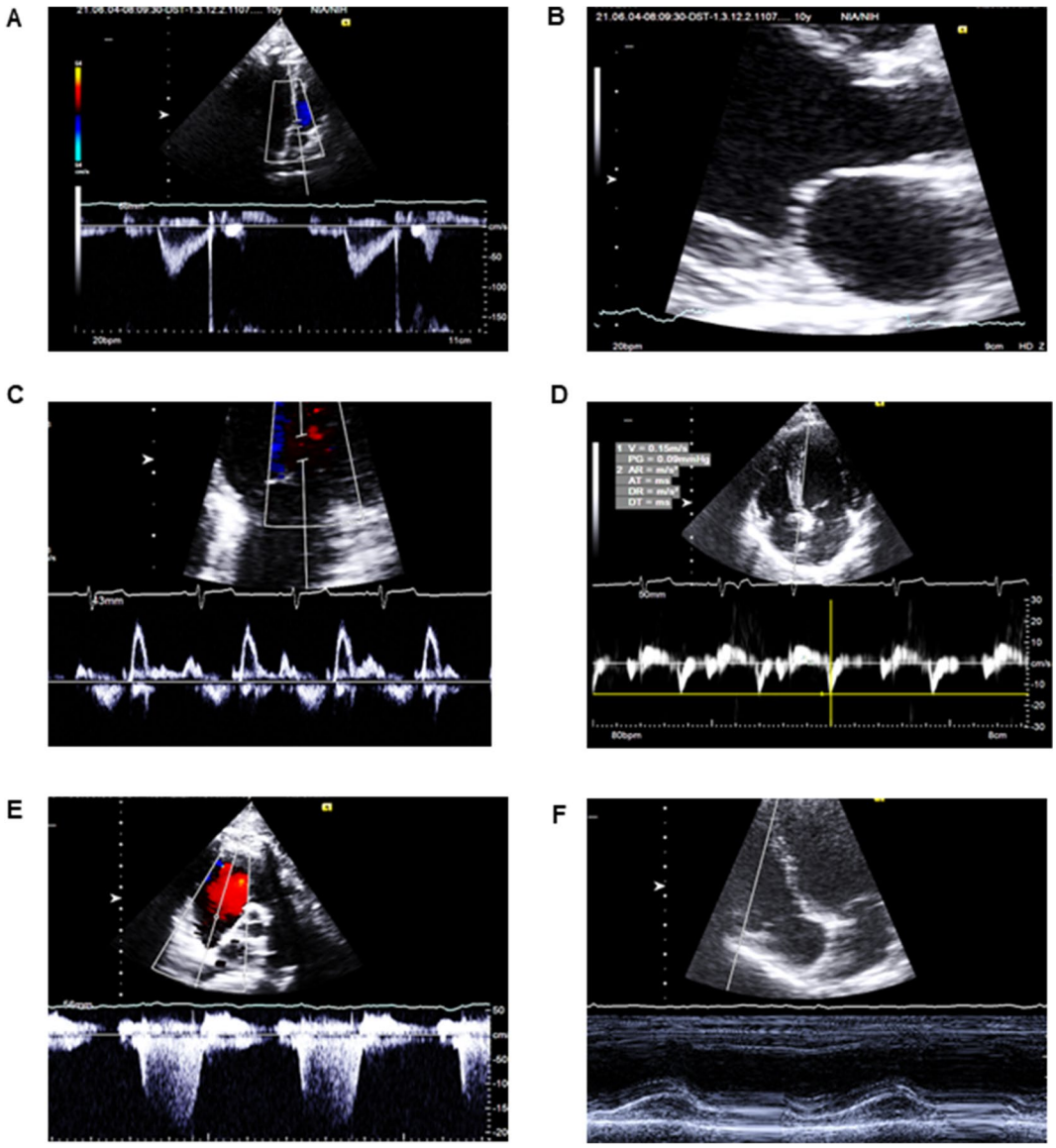

Fig. 2 Comprehensive noninvasive hemodynamic assessment by 2D TTE, M mode, and Doppler. **A** Pulsed wave Doppler of the LV outflow tract. **B** Measurement of the LVOT diameter. **C** Mitral inflow pattern. **D** Tissue Doppler E' wave of the basal LV septum. **E** Tricuspid regurgitation velocity (continuous was Doppler). **F** TAPSE: Tricuspid Annular Peak Systolic Excursion evaluated from the apical 4 chamber view

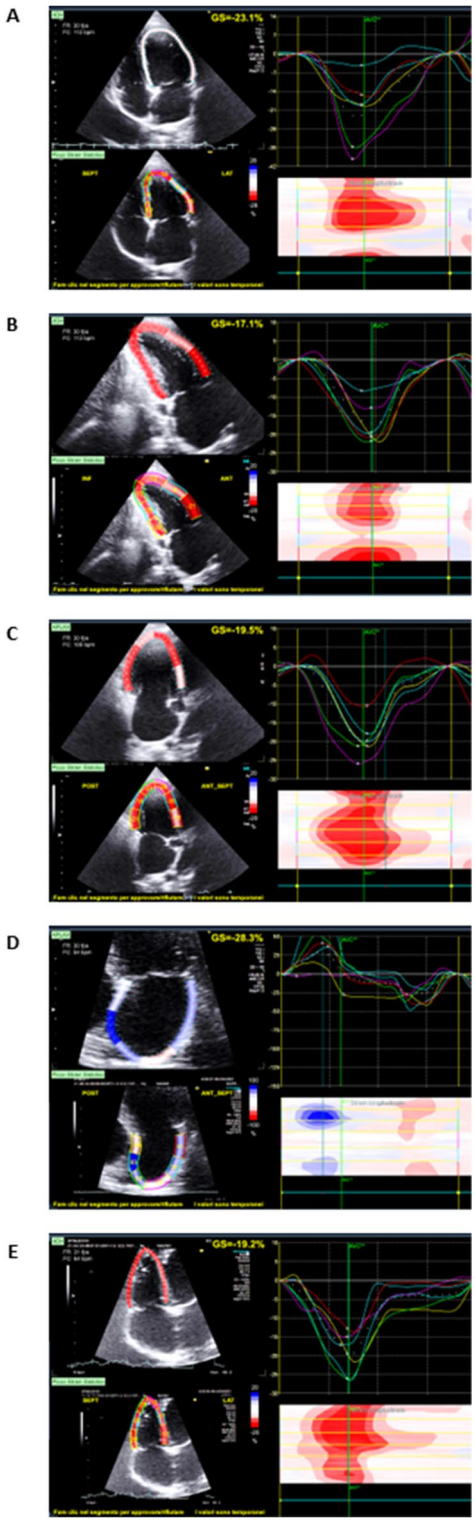

Fig. 3 Examples of strain analysis. **A-C** Left ventricular (LV) strain obtained from the 4 chambers, 2 chambers, and 3 chambers views, respectively. **D** Left atrial strain obtained from a focused 4 chambers. **E** Right ventricular strain from an adapted 4 chambers view. Each analysis allowed quantitative measurements of global longitudinal strain of the chambers and related functional curves

$$AVA(cm^2) = (LVOTvtixLVOTa)/AOvti$$

LV diastolic function was analyzed with mitral valve Pulsed Doppler and mitral annulus tissue Doppler evaluation through the ratio between early (E wave) and late (A wave) pulsed doppler velocities, E wave deceleration time and the ratio between E wave and tissue Doppler early myocardial relaxation velocity (E').

To characterize one aspect of right ventricular (RV) function, tricuspid annular plane systolic excursion (TAPSE) was evaluated by positioning M-mode cursor at the junction of the tricuspid valve plane with the right ventricular free wall in 4 chamber view.

As an index of pulmonary pressures, right ventricular-right atrial gradient was derived from peak velocity of systolic tricuspid regurgitant flow signal by the modified Bernoulli equation [23].

LV global longitudinal (GLS), RV free wall longitudinal (FWLS) strain and left atrial peak longitudinal strain (LAS) were calculated offline from 4 chamber apical view through a dedicated vendor–independent software (EchoPAC, General Electric, v10.8.1).

Myocardial deformation analysis is the underlying principle governing strain. Distinct from displacement, which reflects the change in myocardial fibers' position, deformation reflects the change in dimensions of myocardial fibers over the cardiac cycle. Speckle-tracking echocardiography is a newer modality to assess myocardial deformation and relies on tracking motion of ultrasound 'speckles' over the cardiac cycle. Figure 3 shows examples of strain measurements.

Statistical analysis

RStudio 1.3 running R version 4.0.2 was used to perform all analyses and construct plots.

Two sample t-tests were conducted to compare young vs. old and males vs. females. Graphically,

means with 95% confidence intervals are constructed to compare the four groups.

Two-way ANOVAs were used to analyze each variable. The initial model contained an interaction term between age group and sex. If the interaction was not statistically significant, it was removed and the model with only main effects was fit. Data are reported as mean ± standard deviation, and a p-value of < 0.05 was considered as significant for all analyses.

Results

Body surface area (BSA) did not differ by age (Table 2; Fig. 4A) but did differ by sex, and BSA in females was lower than in males (Table 3, $p = 0.0020$; Fig. 4A).

The heart rate (HR) was significantly higher in old compared to young rhesus monkeys (Table 2, $p = 0.0017$; Fig. 4B) and lower in males than females (Table 3, $p = 0.0079$; Fig. 4B). It is noteworthy that dexmedetomidine, an anesthetic with a beneficial pharmacologic profile [24], similarly to what occurs in humans, decreases the heart rate in NHP. This effect accounts for the heart rate reported herein (86 ± 19 bpm) which is lower than the heart rate in the same monkey population (161 ± 21 bpm; Supplementary Table S2) when NHP underwent anesthesia without Dexmedetomidine, either with Ketamine 7–10 mg/kg IM or Telazol, 3–6 mg/kg, IM, within 6 months of the echocardiographic evaluation reported in this work.

Neither systolic (SBP; Fig. 4C) nor diastolic blood pressure (DBP; Fig. 4D) differed by age (Table 2) and sex (Table 3).

Left ventricle and left atrium structure

Anatomic differences in heart geometry were evaluated by measuring LVEDd, LVESd, LVPW thickness, IVS thickness, LV mass/BSA, LVOTd, AVA, and LAd.

Neither LVEDd nor LVESd differed by age (Table 2; Fig. 5A and B, respectively) but both were larger in males than in females (Table 3, $p = 0.0004$ and $p = 0.0001$ respectively; Fig. 5A and B respectively). Further, LVESd presented an interaction (Table 4, $p = 0.0466$): young females differed from young males and old females differed from old males.

LVPW thickness did not significantly differ by age (Table 2, Fig. 5C) but it was higher in males than in females (Table 3, $p = 0.0069$; Fig. 5C). IVS thickness did not differ by age (Table 2; Fig. 5D) and sex (Table 3; Fig. 5D) but presented an interaction (Table 4, $p = 0.0323$): young females differed from old females and young females differed from young males (Fig. 5D).

LV mass did not differ by age (Table 2) but was higher in males than in females (Table 3; $p = 4.5E\text{-}05$). However, LV mass/BSA differed neither by age (Table 2; Fig. 5E) nor by sex (Table 3; Fig. 5E).

LVOTd was larger in old than in young NHP (Table 2, $p = 0.0258$; Fig. 5F) and in males than females (Table 3, $p = 2.2E\text{-}05$; Fig. 5F). AVA was lower in the young vs old NHP (Table 2, $p = 0.0470$; Fig. 5G) and larger in males than females (Table 3, $p = 0.0017$ Fig. 5G).

LA diameter was larger in males versus females (Table 3; Fig. 5F; $p = 0.0101$) and there were no age-associated differences (Table 2, Fig. 5H).

Left ventricle and left atrium function

Left ventricular systolic function was assessed by Fractional Shortening, Ejection Fraction, Stroke Volume, Stroke Index, Cardiac Output, Cardiac Index, and LV Global Longitudinal Strain (Fig. 6). Fractional shortening differed neither by age nor sex (Tables 2 and 3, respectively; Fig. 6A) Ejection Fraction did not differ by age (Table 2; Fig. 6B) but it was higher in females than in males (Table 3, $p = 0.0237$; Fig. 6B). Stroke Index was higher in old than in young rhesus monkeys (Table 2, $p = 0.0314$; Fig. 6D) and in males than in females (Table 3, $p = 0.0055$; Fig. 6D). However, the heart rate is faster in females than in males (Table 3 and Fig. 4B) and Cardiac Index showed no difference between sexes (Table 3 and Fig. 6F). In contrast, Cardiac Index, similarly to the Stroke Index, is higher in old than in young NHP (Table 2 and Fig. 6F). Finally, age and sex had no effect on LV Global Longitudinal strain (Tables 2 and 3 and Fig. 6G).

Table 2 Descriptive statistics by age

	All			Young			Old			
	n	mean	sd	*n*	mean	sd	*n*	mean	sd	*p*
General Characteristics										
Age (years)	38	15.5	6.9	20	9.3	1.1	18	22.4	2.7	2.3E-15
Body Surface Area (m^2)	33	0.442	0.097	17	0.447	0.110	16	0.436	0.084	0.7289
Heart Rate (bpm)	38	86.3	19.4	20	77.3	16.8	18	96.3	17.5	0.0017
RR interval (ms)	38	731.8	176.4	20	812.3	186.4	18	642.4	113.1	0.0017
Systolic Blood Pressure (mmHg)	33	107.5	17.2	18	105.1	12.6	15	110.5	21.5	0.3997
Diastolic Blood Pressure (mmHg)	33	66.4	12.9	18	64.1	10.7	15	69.1	15.0	0.2831
LV Structure										
LV Mass (g)	38	19.30	6.20	20	18.75	5.57	18	19.92	6.93	0.5723
LV Mass/BSA (g/m^2)	33	42.87	10.98	17	40.74	10.26	16	45.13	11.59	0.2597
LV Diastolic Diameter (cm)	38	2.237	0.339	20	2.220	0.242	18	2.257	0.428	0.7480
LV Diastolic Diameter (cm)/BSA	33	5.185	0.898	17	5.195	0.983	16	5.175	0.830	0.9507
LV Systolic Diameter (cm)	38	1.688	0.371	20	1.724	0.261	18	1.648	0.469	0.5474
LV Posterior Wall Diastolic Thickness (cm)	38	0.486	0.084	20	0.496	0.088	18	0.476	0.080	0.4689
Interventricular Septum Diastolic Thickness (cm)	38	0.473	0.084	20	0.453	0.088	18	0.494	0.074	0.1252
Relative Wall Thickness	38	0.439	0.103	20	0.431	0.083	18	0.448	0.123	0.6324
LVOT Diameter (cm)	38	0.964	0.141	20	0.917	0.135	18	1.017	0.132	**0.0258**
LVOT Area (cm^2)	38	0.745	0.219	20	0.674	0.200	18	0.825	0.215	**0.0317**
LVOT Peak Velocity (cm/s)	38	71.0	11.8	20	74.3	12.7	18	67.4	9.8	0.0665
LVOTvti (cm)	38	10.50	1.67	20	11.11	1.81	18	9.83	1.22	**0.0153**
AV Peak Velocity (cm/s)	38	82.7	16.2	20	88.3	17.7	18	76.6	12.1	**0.0228**
AV Peak Transvalvular Gradient (mmHg)	38	2.80	1.19	20	3.15	1.40	18	2.40	0.75	**0.0466**
AVA (cm^2)	38	0.657	0.212	20	0.593	0.218	18	0.728	0.185	0.0470
LV Systolic Function										
Fractional Shortening (%)	38	0.247	0.108	20	0.224	0.111	18	0.273	0.101	0.1672
LV Ejection Fraction (%)	37	52.4	4.3	20	52.1	4.2	17	52.8	4.5	0.6299
Stroke Volume (ml)	38	6.27	3.79	20	5.57	3.70	18	7.05	3.85	0.2367
Stroke Index (ml/m2)	33	12.50	5.68	17	10.47	5.56	16	14.66	5.12	0.0314
Cardiac Output (ml/min)	38	519.1	282.2	20	401.5	227.4	18	649.7	285.0	0.0059
Cardiac Index (ml/min/m2)	33	1095.1	545.4	17	806.2	399.2	16	1402.0	519.2	0.0010
LV Global Longitudinal Strain (%)	35	19.0	4.8	19	19.7	5.6	16	18.1	3.8	0.3065
LV Diastolic Function										
MV E-wave velocity (cm/s)	38	75.9	17.8	20	80.1	16.0	18	71.3	18.9	0.1288
MV A-wave velocity (cm/s)	38	46.1	14.3	20	39.3	11.0	18	53.7	14.0	0.0013
E/A	38	1.90	0.93	20	2.31	0.93	18	1.43	0.69	0.0020
MV Deceleration Time (ms)	38	101.0	22.8	20	93.3	20.8	18	109.4	22.5	0.0291
Mean e' (cm/s)	38	12.10	2.48	20	12.79	2.23	18	11.33	2.58	0.0733
E/e'	38	6.49	1.47	20	6.57	1.22	18	6.40	1.73	0.7281
Left Atrium										
LA Diameter (cm)	37	1.85	0.29	20	1.82	0.26	17	1.89	0.32	0.4793
LA Diameter (cm)/BSA	32	4.28	0.78	17	4.23	0.92	15	4.34	0.62	0.6692
LA Strain (%)	32	29.81	7.52	18	31.33	9.25	14	27.86	3.96	0.1644
RV Function										
TAPSE (mm)	38	8.67	2.24	20	8.97	2.45	18	8.33	1.99	0.3872
RV Free Wall Longitudinal Strain (%)	35	20.14	4.69	19	20.68	4.29	16	19.50	5.20	0.4755
TR Peak Velocity (cm/s)	37	166.5	21.4	19	161.6	19.7	18	171.7	22.5	0.1592
TR Peak Transvalvular Gradient (mmHg)	37	11.13	2.95	19	10.31	2.56	18	12.00	3.15	0.0838
PV Peak Velocity (cm/s)	37	68.6	14.9	19	70.9	11.7	18	66.2	17.8	0.3517

Diastolic function was evaluated through mitral diastolic flow pattern (E/A ratio), MV Deceleration Time and LA Strain. Young NHP showed an E/A ratio significantly higher than old NHP (Table 2, $p=0.0020$; Fig. 7A), and E/A was higher in male than in female rhesus monkeys (Table 3, $p=0.0406$; Fig. 7A). MV Deceleration Time was higher in old than in young NHP (Table 2, $p=0.0291$; Fig. 7B) and it did not differ between males and female (Table 3; Fig. 7B). MV Deceleration Time presented a significant interaction and young females differed from old females (Table 4, $p=0.0283$; Fig. 7B). Finally, LA Strain did not differ by age (Table 2; Fig. 7C) or sex (Table 3; Fig. 7C).

Right ventricle function

Right Ventricular function was evaluated by measuring the TAPSE and the Right Ventricular FWLS. TAPSE did not differ by age and by sex (Table 2 and 3; Fig. 8A). Right Ventricular FWLS did not differ by age (Tables 2; Fig. 7A), but it was lower in male than in female NHP (Table 3, $p=0.0059$; Fig. 8B).

There were non-statistically significant trends for values of peak velocity of tricuspid regurgitant flow and consequently transvalvular systolic gradient, as indicator of pulmonary pressure, in old versus young and in

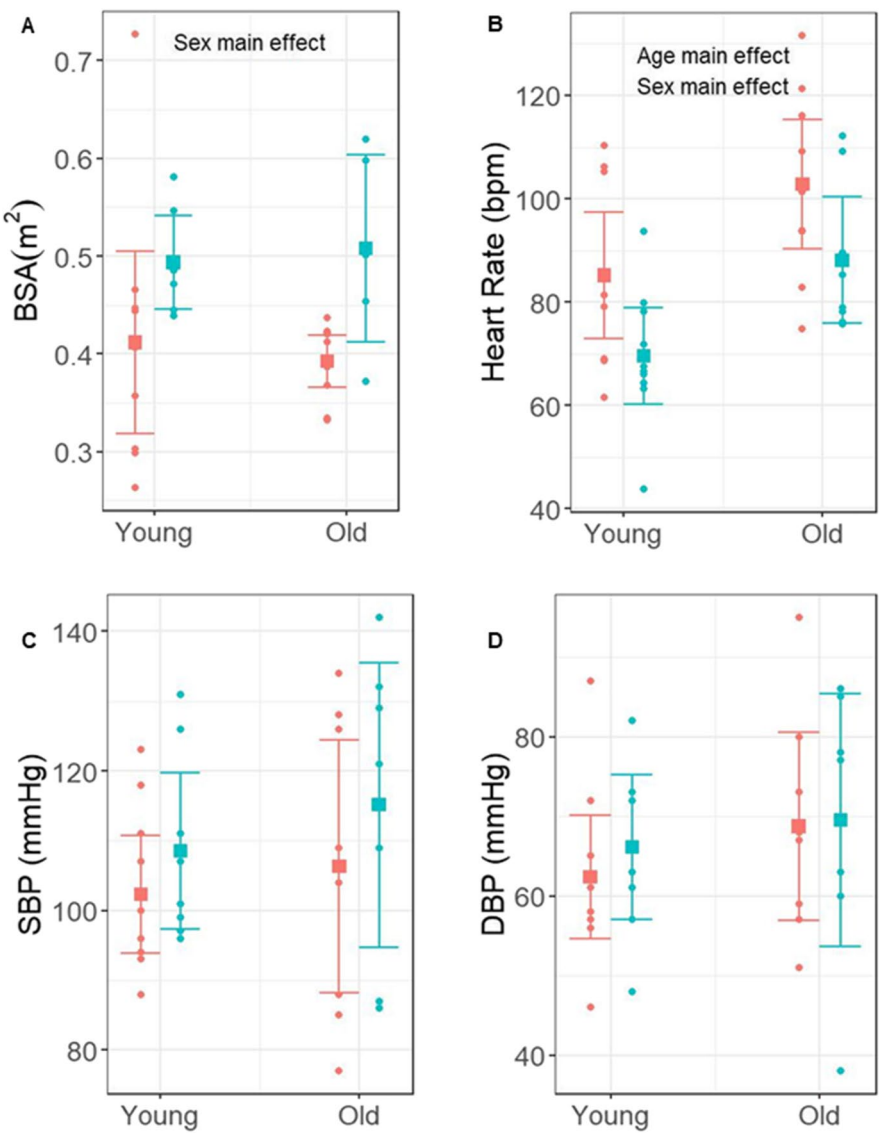

Fig. 4 Cardiovascular parameters. **A** Body surface area (BSA), **B** Heart rate (HR), **C** systolic (SBP), and **D** diastolic blood pressure (DBP) in young and old, female (red) and male (blue) rhesus monkeys. Values are represented as mean and 95% CI

Table 3 Descriptive statistics by sex

	All			Male			Female			*p*
	n	mean	sd	*n*	mean	sd	*n*	mean	sd	
General Characteristics										
Age (years)	38	15.5	6.9	18	15.2	6.8	20	15.8	7.2	0.8172
Body Surface Area (m^2)	33	0.442	0.097	13	0.500	0.070	20	0.404	0.094	**0.0020**
Heart Rate (bpm)	38	86.3	19.4	18	77.8	16.4	20	94.0	19.1	**0.0079**
RR interval (ms)	38	731.8	176.4	18	806.1	185.5	20	665.0	140.8	**0.0134**
Systolic Blood Pressure (mmHg)	33	107.5	17.2	15	111.6	17.6	18	104.1	16.5	0.2203
Diastolic Blood Pressure (mmHg)	33	66.4	12.9	15	67.7	13.7	18	65.2	12.4	0.5895
LV Structure										
LV Mass (g)	38	19.30	6.20	18	23.33	5.57	20	15.68	4.22	**4.5E-05**
LV Mass/BSA (g/m^2)	33	42.87	10.98	13	46.48	7.60	20	40.52	12.32	0.0955
LV Diastolic Diameter (cm)	38	2.24	0.34	18	2.43	0.32	20	2.06	0.25	**0.0004**
LV Diastolic Diameter (cm)/BSA	33	5.185	0.898	13	4.97	0.44	20	5.33	1.09	0.2003
LV Systolic Diameter (cm)	38	1.69	0.37	18	1.91	0.32	20	1.49	0.29	**0.0001**
LV Posterior Wall Diastolic Thickness (cm)	38	0.486	0.084	18	0.523	0.070	20	0.453	0.083	**0.0069**
Interventricular Septum Diastolic Thickness (cm)	38	0.473	0.084	18	0.491	0.086	20	0.456	0.079	0.2022
Relative Wall Thickness	38	0.439	0.103	18	0.429	0.114	20	0.448	0.094	0.5702
LVOT Diameter (cm)	38	0.964	0.141	18	1.059	0.127	20	0.879	0.089	**2.2E-05**
LVOT Area (cm^2)	38	0.745	0.219	18	0.893	0.207	20	0.612	0.123	**2.9E-05**
LVOT Peak Velocity (cm/s)	38	71.0	11.8	18	70.6	11.5	20	71.4	12.3	0.8376
LVOTvti (cm)	38	10.50	1.67	18	10.64	1.48	20	10.38	1.85	0.6222
AV Peak Velocity (cm/s)	38	82.7	16.2	18	85.4	15.3	20	80.3	17.0	0.3370
AV Peak Transvalvular Gradient (mmHg)	38	2.80	1.19	18	2.92	1.17	20	2.69	1.22	0.5635
AVA (cm^2)	38	0.657	0.212	18	0.768	0.215	20	0.557	0.155	**0.0017**
LV Systolic Function										
Fractional Shortening (%)	38	0.247	0.108	18	0.217	0.082	20	0.274	0.123	**0.0995**
LV Ejection Fraction (%)	37	52.4	4.3	18	50.8	4.8	19	54.0	3.2	**0.0237**
Stroke Volume (ml)	38	6.27	3.79	18	8.84	3.92	20	3.96	1.53	**6.3E-05**
Stroke Index (ml/m2)	33	12.50	5.68	13	16.05	5.82	20	10.20	4.34	**0.0055**
Cardiac Output (ml/min)	38	519.1	282.2	18	674.3	294.7	20	379.4	184.5	**0.0011**
Cardiac Index (ml/min/m2)	33	1095.1	545.4	13	1266.0	554.6	20	984.0	523.2	0.1571
LV Global Longitudinal Strain (%)	35	18.97	4.84	17	17.91	4.16	18	19.97	5.32	0.2097
LV Diastolic Function										
MV E-wave velocity (cm/s)	38	75.9	17.8	18	78.9	17.4	20	73.3	18.1	0.3356
MV A-wave velocity (cm/s)	38	46.1	14.3	18	40.3	13.3	20	51.3	13.5	**0.0166**
E/A	38	1.896	0.928	18	2.230	1.105	20	1.595	0.618	**0.0406**
MV Deceleration Time (ms)	38	101.0	22.8	18	99.7	17.9	20	102.1	27.0	0.7414
Mean e' (cm/s)	38	12.10	2.48	18	12.91	2.50	20	11.37	2.28	0.0570
E/e'	38	6.49	1.47	18	6.15	1.35	20	6.81	1.53	0.1671
Left Atrium										
LA Diameter (cm)	37	1.853	0.290	18	1.981	0.347	19	1.732	0.151	**0.0101**
LA Diameter (cm)/BSA	32	4.28	0.78	13	3.965	0.493	19	4.497	0.880	**0.0373**
LA Strain (%)	32	29.81	7.52	15	28.07	6.93	17	31.35	7.89	0.2195
RV Function										
TAPSE (mm)	38	8.67	2.24	18	9.37	2.00	20	8.03	2.30	0.0622
RV Free Wall Longitudinal Strain (%)	35	20.14	4.69	17	17.95	4.57	18	22.21	3.88	**0.0059**
TR Peak Velocity (cm/s)	37	166.5	21.4	17	169.0	23.2	20	164.5	20.2	0.5367
TR Peak Transvalvular Gradient (mmHg)	37	11.1	2.9	17	11.6	3.2	20	10.7	2.7	0.3865
PV Peak Velocity (cm/s)	37	68.6	14.9	17	68.9	12.8	20	68.3	16.8	0.9028

male versus female rhesus monkeys (Tables 2 and 3; Fig. 8C).

Discussion

Appropriate reference ranges are essential to identify cardiac abnormalities that develop in a variety of physiologic and pathologic conditions. This is the first study to provide the complete echocardiographic evaluation of cardiac structure, and systolic and diastolic function, including atrial and ventricular strains, and their age- and sex-related differences, in a cohort of healthy rhesus macaques, validating these NHP as a reliable animal model of human cardiovascular aging.

Our data were collected in healthy, adult rhesus monkeys with a consistent body surface area, a variable that did not change between young and old NHP. Moreover, in our NHP population, we found no evidence of other CV diseases that are frequently present in old humans, e.g., aortic stenosis, mitral annular calcification, cardiac amyloidosis. It is noteworthy that in the present study AVA did not decrease as a function of age, and that the peak AV velocity and transvalvular gradient did not increase in old vs young NHP. This is in contrast with the increased prevalence of aortic stenosis in old vs young human subjects. The mechanisms underlying the development of calcific aortic stenosis in humans have not been fully elucidated; however, the development of aortic stenosis is associated with several risk factors including genetic predisposition, altered calcium metabolism, diabetes and metabolic syndrome, hypertension, hyperlipidemia, elevated Lp(a) levels, smoking [25, 26]. These risk factors either were not present in our NHP cohorts, or the animals were not tested for them, e.g. Lp(a). Therefore, the absence or very low prevalence of risk factors for aortic stenosis in our old NHP population likely accounts for the absence of aortic stenosis in the old NHP included in the present work.

The main novelty of this study is the detailed echo-Doppler analysis of cardiac structure and systolic and diastolic functional parameters, including left ventricular GLS, right ventricular FWLS and LAS. Neither systolic nor diastolic blood pressure differed significantly by age group or sex, therefore, cardiac structure and function reflect mainly aging and were not affected by differences in blood pressure. The main findings of our study are: 1) heart chamber dimensions did not differ between young and old but were higher in males than females; 2) LVPW thickness and LV mass did not differ by age group but were higher in males than females; 3) systolic function was assessed by different parameters: both stroke index and cardiac index were higher in old than in young rhesus monkeys; ejection fraction and stroke index were higher in females than in males whereas stroke volume was higher in males than in females; interestingly, left ventricular GLS did not differ by age and sex; 4) E/A is a main index of diastolic function and decreased in old vs young NHP; further MV deceleration time was prolonged in old compared to young female rhesus monkeys; 5) advanced echo-Doppler parameters, including strain of both ventricles and of the left atrium in rhesus monkey were very similar to those in humans. Taken together, our results show that most anatomical and functional age-associated [27] and sex-associated [28] differences in rhesus monkey heart are similar to what is found in humans and validate rhesus macaques as an excellent animal model to study human cardiovascular aging, both in females and males.

Among the echocardiography indices, LVEF and the E/A ratio of early to late trans-mitral Doppler inflow velocity (E/A) are commonly used to evaluate LV function in risk assessment of heart failure and cardiac death. Subtle changes in both systolic and diastolic function of the LV and LA, however, may be better described by GLS and LAS in association with a detailed structural and functional analysis of heart chambers. In humans, changes in GLS of the LV may precede LVEF changes in several diseases, including diabetes and hypertension. Importantly, GLS of both ventricles may better define age- and sex-associated changes of systolic function because it is a sensitive indicator that can be affected by subtle functional changes. In this regard, we utilized a dedicated commercial software to analyze GLS of the LV as well as the free wall of the RV and LA.

Left ventricular systolic function

In previous NHP studies [16, 29, 30] and in most studies of human populations [16, 17, 31], LV systolic function was assessed only by LVFS or LVEF;

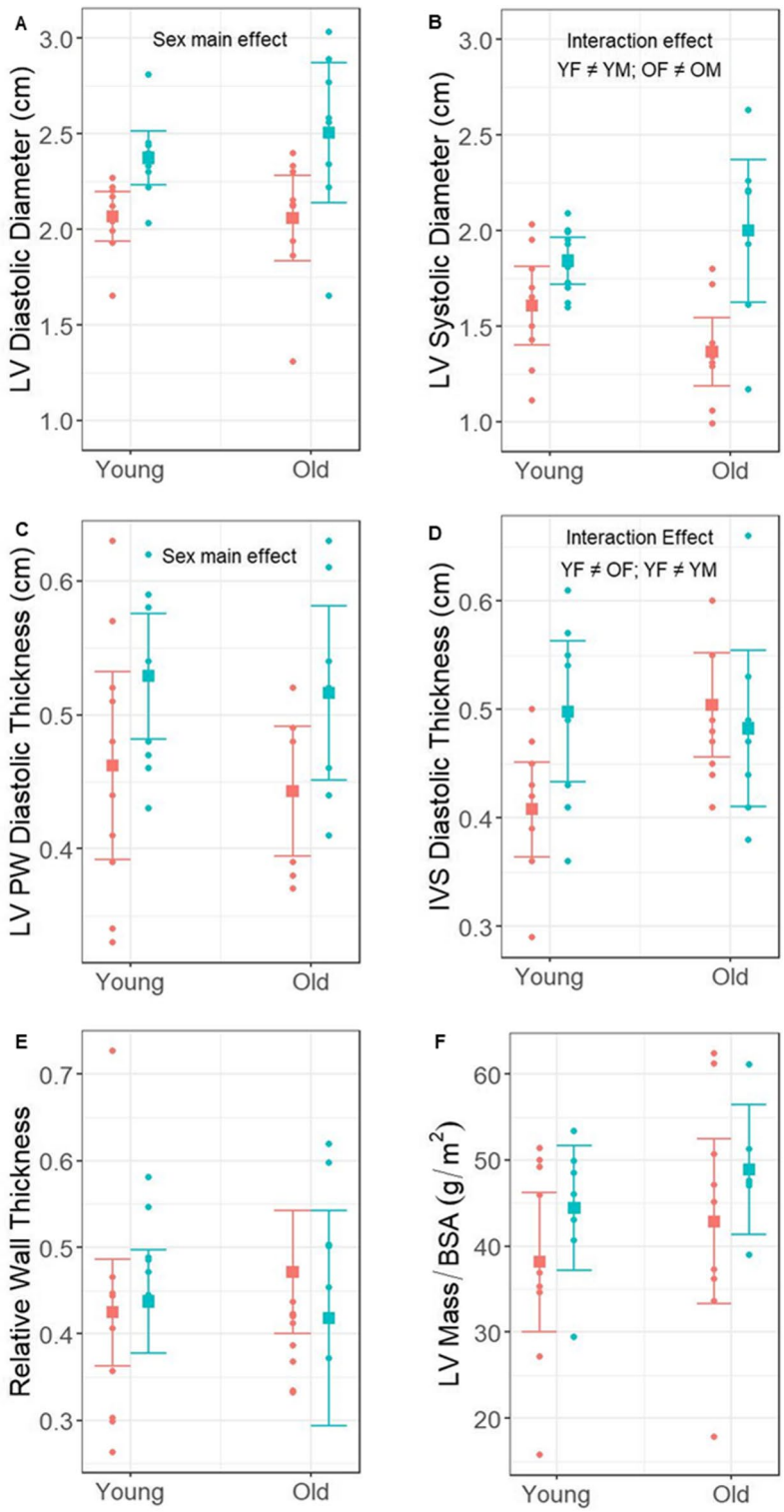

Fig. 5 Cardiac structure. M-mode measurements in young and old, female (red) and male (blue) rhesus monkeys of LV diameters in **A** diastole and **B** systole, **C** posterior wall (PW) diastolic thickness, **D** interventricular septum (IVS) diastolic thickness, **E** Relative Wall Thickness, **F** LV mass normalized to BSA, **G** LV Outflow Tract (LVOT) diameter, **H** Aortic Valve Area (AVA) measured from 5 chamber apical view, **I** Left Atrium (LA) Systolic diameter**.** Values are represented as mean and 95% CI

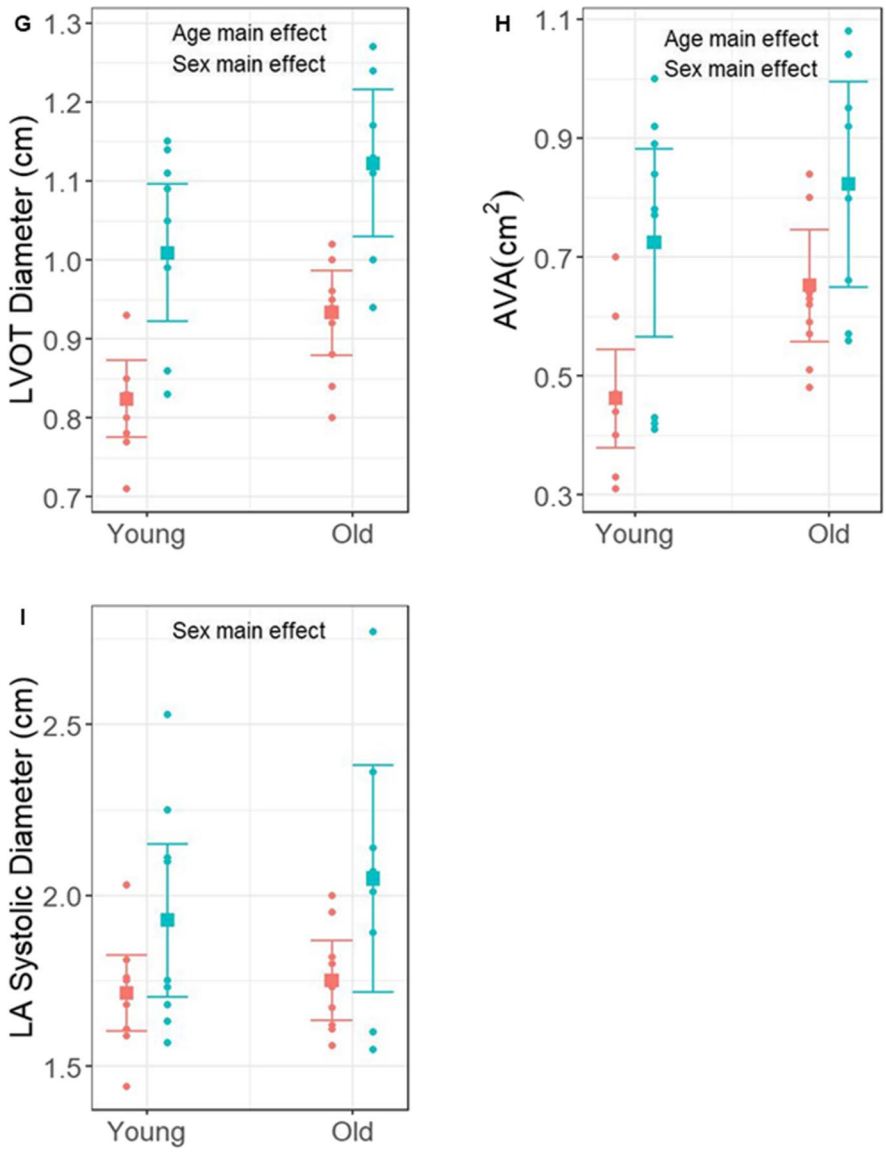

Fig. 5 (continued)

in contrast, we also calculated stroke volume, stroke index, cardiac output, cardiac index, and GLS from 4- chamber apical view, thus obtaining a more accurate LV function estimate. In the absence of regional wall motion abnormalities, as it was the case in NHPs included in the present study, left ventricular GLS calculated only from the apical 4-chamber view is comparable to the strain value obtained including anterior wall, inferior wall, inferoseptal wall, and the anteroseptum.

LVFS, LVEF, stroke volume and left ventricular GLS did not differ by age, however, left ventricular GLS exhibited a trend to suggest a worse function in old vs young rhesus monkeys (-18.1 vs -19.7 respectively, $p = 0.3065$); in contrast, cardiac output, because of the faster heart rate in old vs young, was higher in old than in young NHP.

The effect of sex on left ventricular systolic function yielded contrasting results among the different parameters; LVFS and left ventricular GLS showed no sex effect, however there was a trend of left ventricular GLS to suggest a better function in females vs males (-20.0 vs -17.9 respectively; $p = 0.2097$), LVEF was higher in females vs males, whereas stroke volume, stroke index and cardiac output were higher in males than in females. However, males have a higher

Table 4 *p*-values from full and reduced ANOVA models

	Full model (with interaction)			Model with only main effects	
	Age group	Sex	Interaction	Age group	Sex
General Characteristics					
Body Surface Area (m^2)	0.6226	0.0166	0.5944	0.8367	**0.0036**
Heart Rate (bpm)	0.0171	0.0571	0.9244	**0.0010**	**0.0048**
RR interval (ms)	0.0498	0.1668	0.4752	**0.0013**	**0.0074**
Systolic Blood Pressure (mmHg)	0.6240	0.3366	0.8344	0.3861	0.2261
Diastolic Blood Pressure (mmHg)	0.3187	0.9051	0.7562	0.2776	0.6013
LV Structure					
LV mass (g)	0.4377	0.0029	0.9248	0.3222	**2.5E-05**
LV Mass/BSA (g/m^2)	0.3390	0.2911	0.9752	0.2235	0.1162
LV Diastolic Diameter (cm)	0.9512	0.0026	0.4647	0.5416	0.0003
LV Diastolic Diameter (cm)/BSA	0.9060	0.4866	0.9500	0.9181	0.2777
LV Systolic Diameter (cm)	0.0783	7.1E-05	**0.0466**		
LV Posterior Wall Diastolic Thickness (cm)	0.5920	0.0574	0.9035	0.5279	0.0088
Interventricular Septum Diastolic Thickness (cm)	0.0083	0.5580	**0.0323**		
Relative Wall Thickness	0.3249	0.2869	0.3381	0.6503	0.5879
LVOT Diameter (cm)	0.0154	0.0002	0.9428	**0.0009**	**5.6E-07**
LVOT Area (cm^2)	0.0284	0.0001	0.7333	**0.0012**	**5.8E-07**
LVOT Peak Velocity (cm/s)	0.8756	0.1338	0.0801	0.0715	0.7542
LVOT VTI (cm)	0.3081	0.5987	0.2806	0.0195	0.7008
AV Peak Velocity (cm/s)	0.2469	0.9113	0.4997	**0.0288**	0.3773
AV Peak Transvalvular Gradient (mmHg)	0.2481	0.9328	0.7335	0.0576	0.6243
AVA (cm^2)	0.0192	0.0454	0.4219	**0.0128**	**0.0004**
LV Systolic Function					
Fractional Shortening (%)	0.0317	0.0200	0.0810	0.1885	0.1184
LV Ejection Fraction (%)	1.0000	0.2209	0.6492	0.6556	**0.0237**
Stroke Volume (ml)	0.2037	0.0006	0.9111	0.0638	**4.3E-06**
Stroke Index (ml/m^2)	0.0373	0.0171	0.9749	**0.0084**	**0.0007**
Cardiac Output (ml/min)	0.0159	0.0012	0.6235	**0.0003**	**4.4E-05**
Cardiac Index ($ml/min/m^2$)	0.0047	0.2159	0.9448	**0.0004**	0.0621
LV Global Longitudinal Strain (%)	0.2003	0.6989	0.4810	0.2639	0.1795
LV Diastolic Function					
MV E-wave velocity (cm/s)	0.1437	0.3034	0.5588	0.1389	0.3714
MV A-wave velocity (cm/s)	0.0003	0.0028	0.0810	**0.0007**	**0.0103**
E/A	0.0080	0.0524	0.5561	**0.0020**	**0.0262**
MV Deceleration Time (ms)	0.0023	0.0768	**0.0283**		
Mean e' (cm/s)	0.0297	0.0260	0.1854	0.0770	0.0607
E/e'	0.9593	0.1873	0.5951	0.6629	0.1682
Left Atrium					
LA Diameter (cm)	0.7720	0.0294	0.6329	0.3830	0.0070
LA Diameter (cm)/BSA	0.7997	0.2277	0.9255	0.6796	0.0622
LA Strain (%)	0.0225	0.6012	0.0616	0.1653	0.1834
RV Function					
TAPSE (mm)	0.3147	0.0911	0.5160	0.4347	0.0722
RV Free Wall Longitudinal Strain (%)	0.9250	0.0086	0.3233	0.2833	0.0044

Table 4 (continued)

	Full model (with interaction)			Model with only main effects	
	Age group	Sex	Interaction	Age group	Sex
TR Peak Velocity (cm/s)	0.7804	0.1956	0.2493	0.1553	0.4985
TR Peak Transvalvular Gradient (mmHg)	0.5175	0.1693	0.3187	0.0775	0.3369
PV Peak Velocity (cm/s)	0.7436	0.3094	0.1359	0.3537	0.9268

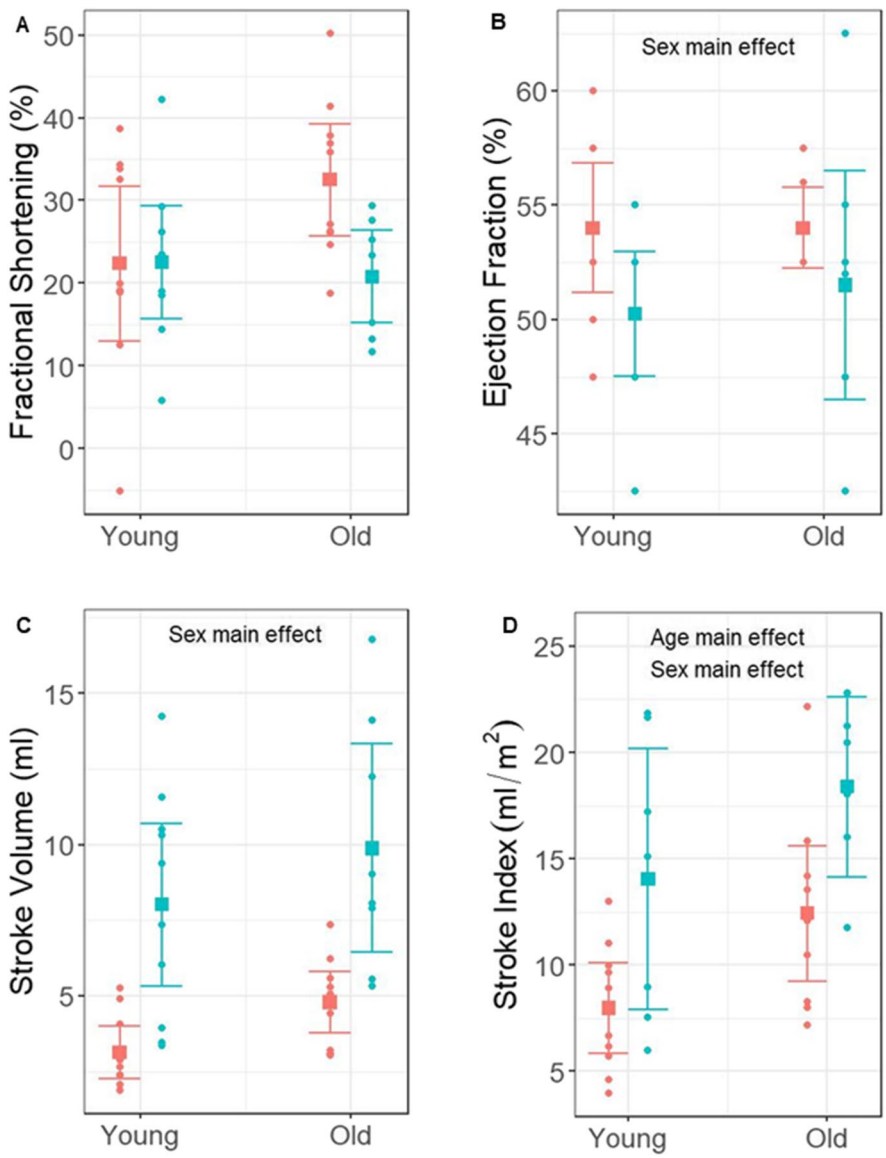

Fig. 6 Left ventricle function. M-mode measurements in young and old, female (red) and male (blue) monkeys of **A** Fractional shortening, **B** Ejection Fraction, **C** Stroke volume and **D** Stroke Index, **E** Cardiac Output, **F** Cardiac Index, and **G** LV Global Longitudinal Strain. Values are represented as mean and 95% CI

Fig. 6 (continued)

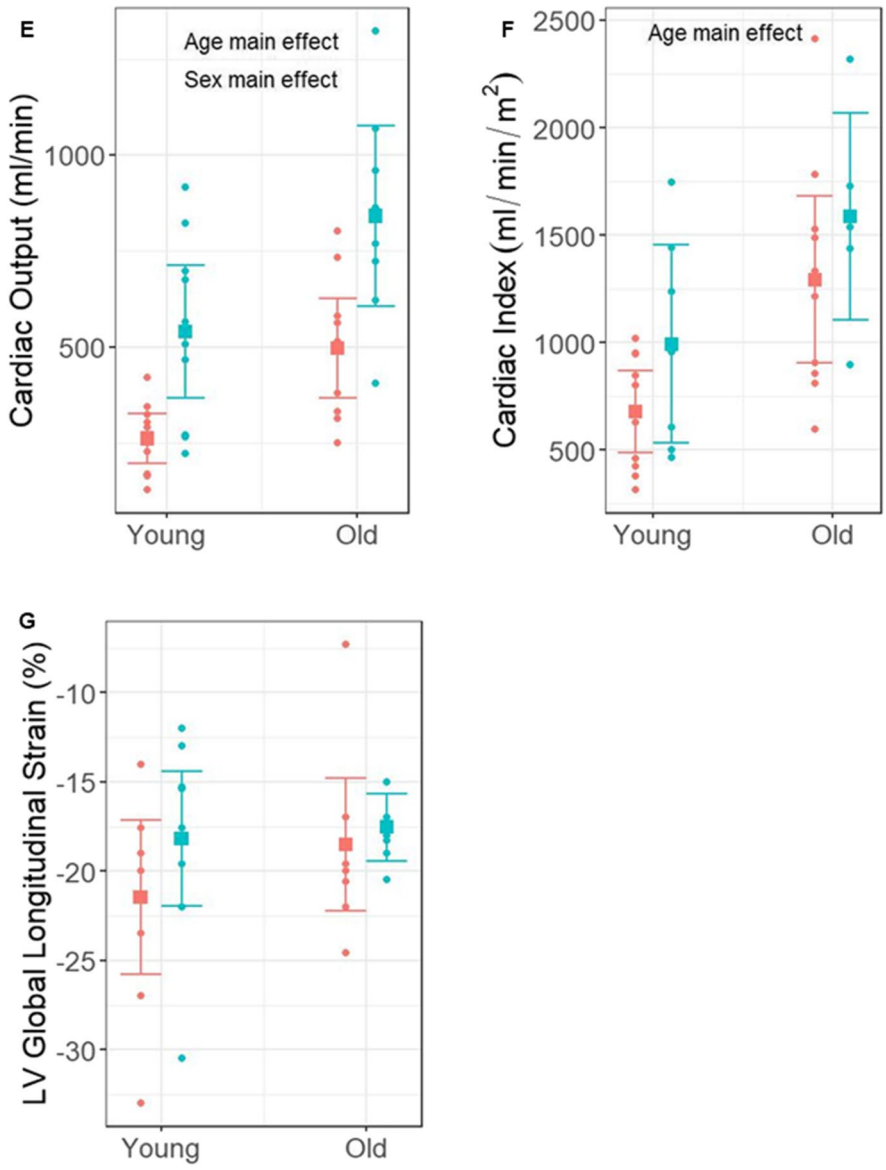

BSA than females and females have a faster heart rate than males; cardiac index is a parameter that normalizes stroke volume, i.e., the amount of blood ejected from the left ventricle with each contraction, to heart rate and BSA, and it showed no effect of sex.

Right ventricular systolic function

Right ventricular systolic function was analyzed by TAPSE and by FWLS and neither of these parameters differed by age although both exhibited a trend to suggest a better RV performance in young vs old NHP (TAPSE 8.97 vs 8.33 mm and RV FWLS – 20.7 vs -19.5, respectively). Further, TAPSE exhibited no sex effect, but FWLS demonstrated a better RV performance in females vs males. These results are novel and similar to what is found in humans [21].

To the best of our knowledge, this is a new important finding suggesting that both ventricles, as expected in the absence of pathologic conditions, had a normal systolic interdependence in the presence of normal arterial and pulmonary systolic pressures. Indeed, in our population the systolic pressures of both arterial and pulmonary circulation were not

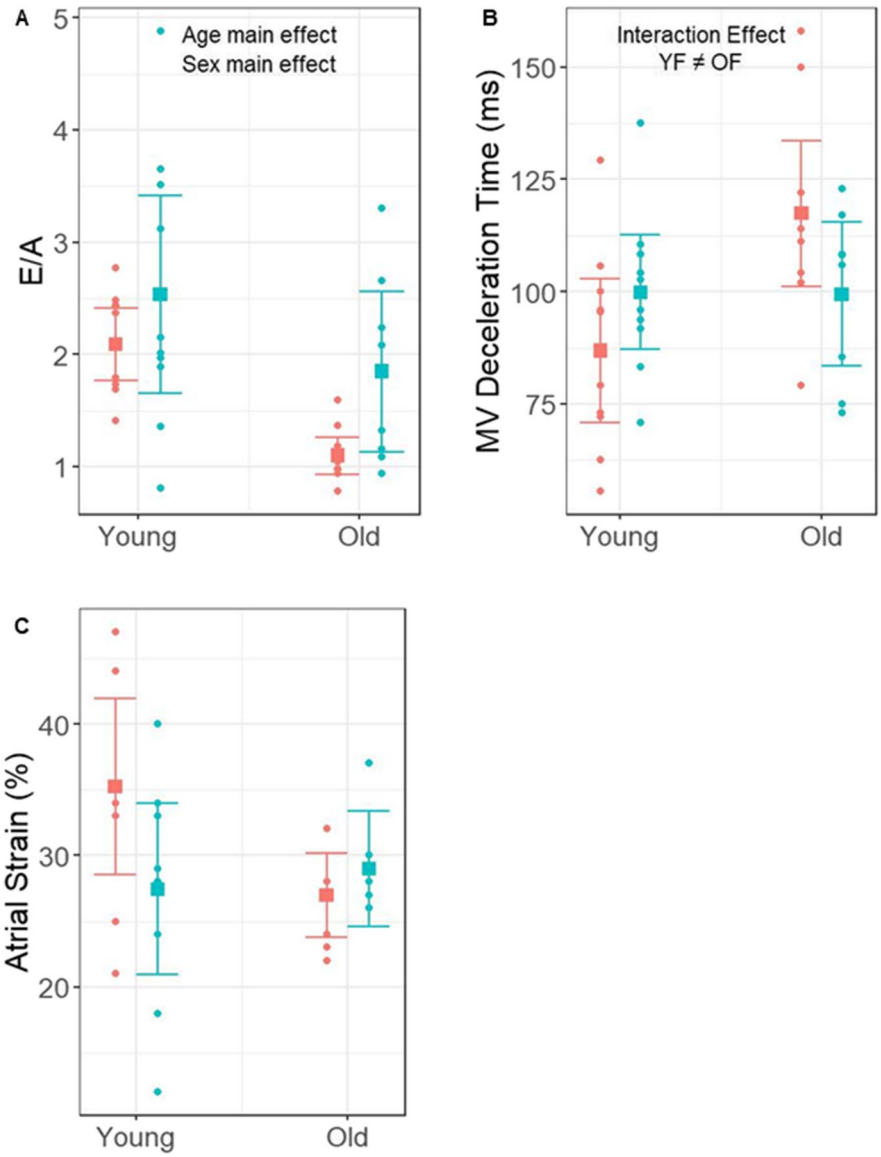

Fig. 7 Diastolic function. **A** E/A ratio, **B** Mitral Valve (MV) Deceleration time, and **C** Atrial Strain was analyzed with mitral valve Pulsed Doppler and mitral annulus tissue Doppler in young and old, female (red) and male (blue) rhesus monkeys. Values are represented as mean and 95% CI

different with aging and therefore the contribution of ventricular contractility to the contractility of the other ventricle (systolic interdependence) did not affect LV and RV systolic function.

Diastolic function

Changes in diastolic function underlie HFpEF, the most common form of HF in the elderly, and were specifically addressed in the present work. In order to better evaluate diastolic function, we included dexmedetomidine in the anesthesia protocol. Dexmedetomidine is a centrally acting selective α_2 adrenoceptor agonist with anesthetic and sedative properties that is known to decrease the heart rate in humans and NHP [32]. This effect accounts for the heart rate reported herein (86 ± 19 bpm) which is lower than the heart rate in the same monkey population (161 ± 21 bpm) when NHP underwent standard anesthesia without Dexmedetomidine. In the presence of tachycardia and of a short diastolic time interval, E/A waves, deceleration time (DT), tissue doppler echocardiography (DTI), and strain values are more difficult to evaluate and interpret

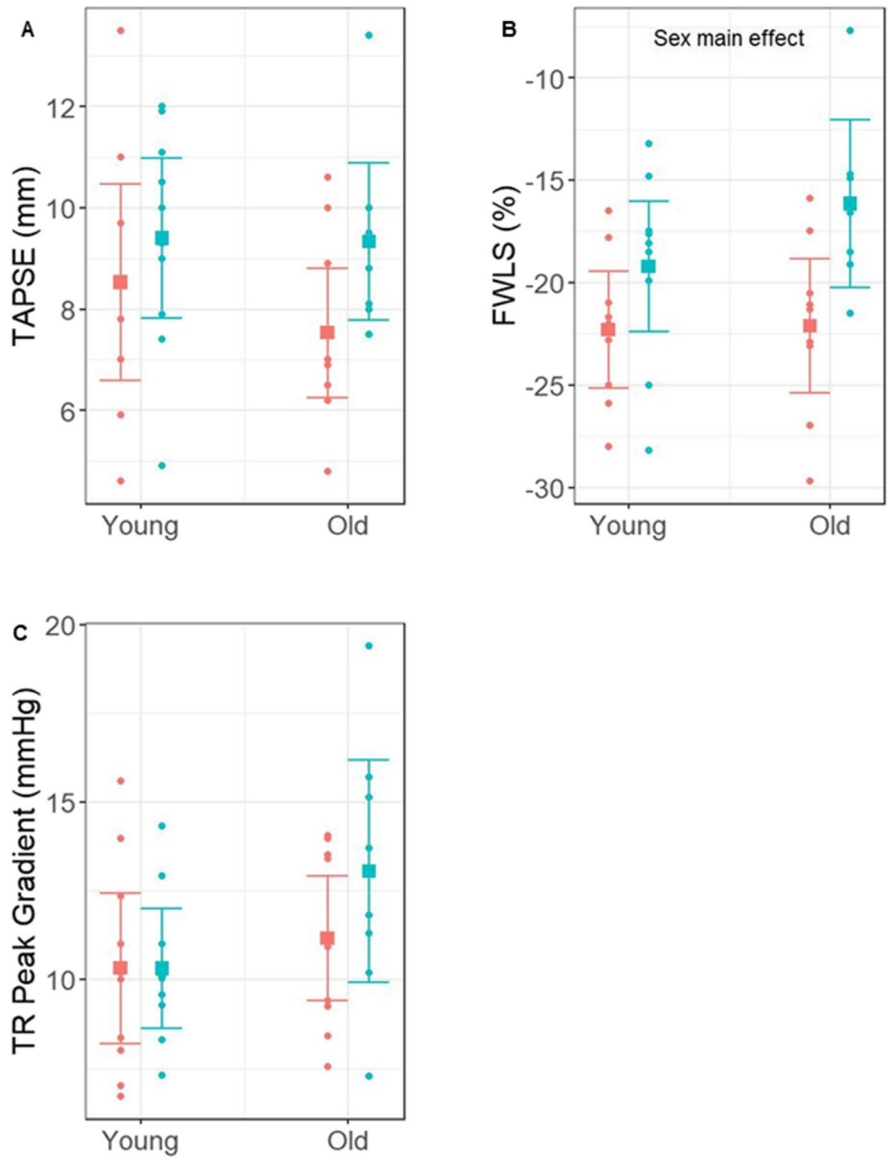

Fig. 8 Right ventricle function. **A** Measurements of tricuspid annular plane systolic excursion (TAPSE) in M-mode. **B** Right ventricular free wall longitudinal (FWLS) strain was calculated from 4 chamber apical view and **C** Pulmonary artery pressures were estimated by the Tricuspid regurgitation (TR) peak gradient in young and old, female (red) and male (blue) rhesus monkeys. Values are represented as mean and 95% CI

than at lower heart rates. Therefore, the use of Dexmedetomidine enabled us to measure several important echocardiographic parameters more accurately. Prior studies have shown LV diastolic dysfunction in NHP models of dysmetabolism and diabetes [33–35] or hypertension [36, 37]. In contrast, our aim was to evaluate diastolic parameters in healthy monkeys, and we found, in accordance with other NHP studies [15, 16], that diastolic indexes derived by the mitral flow pattern and LA dimensions were age- and sex-related. The effect of age on diastolic function in humans was initially shown in subjects 25 to 84 years of age without evidence of cardiovascular disease by the reduction of the E–F slope of the anterior mitral valve leaflet [27]. Mantero et al. [38] described LV diastolic parameters in 288 normal human subjects from 20 to 80 years of age; with aging, doppler E wave velocity decreased, E wave deceleration time increased, A wave velocity increased, and E/A ratio decreased. Interestingly, they demonstrated that E/A ratio reached a value of 1 at approximately 65 years of age and inverted in those over 70 years old. In agreement with what has been described in humans, we found a decrease in E/A ratio in old vs

young rhesus monkeys, both males and females, but an inversion of the E/A ratio in the older group was not evident, possibly because we did not evaluate older NHP. Further, we found that deceleration time was prolonged in old vs young females. LA systolic diameter was higher in males vs females but exhibited no age-dependent difference. Nakayama et al. [29] studied a large population of cynomolgus monkeys grouped as immature (age < 8 years old), mature (≥ 8 to < 20 years old), and elderly (> 20 years old). They showed that the E/A ratio decreased with age. Indeed, E/A ratio varied in each age group but remained within the normal range for humans and other NHP. In our study, we did not include immature monkeys, but only young adults (9.3 ± 1.1 years old) and older NHP (22.4 ± 2.7 years old).

Old NHP exhibited a slight increase in LA area and decrease in LAS and DTI e' velocity without statistical differences compared to young NHP; E/e', a parameter highly associated with LV filling pressure, did not differ between the two age groups. Altogether our data suggest that old monkeys had initial diastolic dysfunction without increase in LA pressures and that LA remodeling may follow.

Diastolic function was also sex related: E/A ratio was significantly lower in females than in males, LV cavity dimensions was smaller and relative wall thickness (ratio between thickness and radius) was higher in females and these structural differences may explain sex differences in the MV inflow patterns. Notably, HFpEF is frequently more common in females compared to males. However, in humans the interaction of sex and age has rarely been analyzed in detail, and knowledge of the distinction between pre- and post-menopausal women is lacking.

Our results are in general agreement with a recent study that examined the effect of age and sex on echocardiographic parameters in rhesus monkeys aged 6 months to 30 years with body weights ranging from 1.4 to 22.6 kg [17]. This study included very young NHP, still in the early developmental phases of life, whereas we compared adult vs old rhesus monkeys (7–30 years old). Differences in the endpoints analyzed in our study were not as pronounced as when a wider age range was used and included NHP in the developmental phase of life. Moreover, in agreement with human echocardiography studies, some of our analyses were correlated to the BSA, a parameter that, unlike the body weight utilized for normalization in the paper by Ueda et al., did not change with aging across the age range we studied.

In summary, our work represents the first detailed study to examine by echocardiography the morphometry and the function of the heart in young and old rhesus macaques of both sexes by including LV GLS, RV FWLS, and LAS, in addition to stroke volume, stroke index, cardiac output and cardiac index as well as the standard measurements of LVFS and LVEF. The results show that cardiovascular changes that occur with age in rhesus macaques mimic the effect of aging in humans, both in males and females, and provide a reference for future studies of cardiac function that will address the effect of diseases, such as diabetes and hypertension, in young and old NHP of both sexes.

Abbreviations **AVA: Aortic Valve Area; BSA: Body Surface Area; DBP: Diastolic Blood Pressure; EF: Ejection Fraction; FS: Fractional Shortening; FWLS: Right Ventricular Free Wall Longitudinal Strain; GLS: Left Ventricular Global Longitudinal Strain; HF: Heart Failure; HFpEF: Heart Failure with preserved Ejection Fraction; HFrEF: Heart Failure with reduced Ejection Fraction; HR: Heart Rate; IVS: Interventricular Septum; LA: Left Atrium; LAS: Left Atrial Strain; LV: Left Ventricle; LVEDV: LV End Diastolic Volume; LVESV: LV End Systolic Volume; LVOT: Left Ventricular Outflow Diameter; MV: Mitral Valve; NHP: Non-Human Primates; PV: Pulmonary Valve; PW: Posterior Wall; RV: Right Ventricle; SBP: Systolic Blood Pressure; TAPSE: Tricuspid Annular Plane Systolic Excursion; TR: Tricuspid Regurgitation**

Acknowledgements The authors would like to thank the NIH Fellow Editorial Board for their editorial assistance and the NIA Nonhuman Primate Core research team.

Funding This project was supported by the Intramural Research Program of the NIH, National Institute on Aging NIA, NIH, Baltimore, MD.

Data availability Data will be made available via supplemental material or an online data repository at the time of associated publication or as soon as possible after publication date. Harvard Dataverse is a free data repository open to all researchers from any discipline, both inside and outside of

the Harvard community, where you can share, archive, cite, access, and explore research data. Harvard Dataverse is supported by Harvard Library and Harvard University Information Technology. Procedures are in place to ensure dataset preservation include storage of data files in multiple geographic locations, regular audits for fixity and authenticity, and succession plans in the event of repository closure https://dataverse.harvard.edu/.

Declarations

Conflict of interest The authors declare that the research was conducted in the absence of any commercial or financial relationships that could be construed as a potential conflict of interest.

References

1. United Nations, D.o.E.a.S.A., Population Division, World Population Ageing 2019: Highlights *(*in *(ST/ESA/SER.A/430).* (ST/ESA/SER.A/430). Editor. 2019, United Nations, Department of Economic and Social Affairs, Population Division
2. Withaar C, et al. Aging and HFpEF: Are we running out of time? J Mol Cell Cardiol. 2022;168:33–4.
3. Savarese G, Becher PM, Lund LH, Seferovic P, Rosano GMC, Coats AJS. Global burden of heart failure: a comprehensive and updated review of epidemiology. Cardiovasc Res. 2023;118(17):3272–87. https://doi.org/10.1093/cvr/cvac013.
4. Magnussen C, et al. Sex-specific epidemiology of heart failure risk and mortality in Europe: Results from the biomarcare consortium. JACC Heart Fail. 2019;7(3):204–13.
5. van Ommen AMLN, et al. Diastolic dysfunction and sex-specific progression to HFpEF: current gaps in knowledge and future directions. BMC Med. 2022;20(1):496.
6. Tsao CW, et al. Temporal trends in the incidence of and mortality associated with heart failure with preserved and reduced ejection fraction. JACC Heart Fail. 2018;6(8):678–85.
7. Pfeffer MA, Shah AM, Borlaug BA. Heart Failure with preserved ejection fraction in perspective. Circ Res. 2019;124(11):1598–617.
8. Owan TE, et al. Trends in prevalence and outcome of heart failure with preserved ejection fraction. N Engl J Med. 2006;355(3):251–9.
9. Phillips KA, et al. Why primate models matter. Am J Primatol. 2014;76(9):801–27.
10. Roth GS, et al. Aging in Rhesus Monkeys: Relevance to human health interventions. Science. 2004;305(5689):1423–6.
11. Mattison JA, Vaughan KL. An overview of nonhuman primates in aging research. Exp Gerontol. 2017;94:41–5.
12. Korcarz CE, et al. Doppler echocardiographic reference values for healthy rhesus monkeys under ketamine hydrochloride sedation. J Med Primatol. 1997;26(6):287–98.
13. Tsusaki H, et al. Evaluation of cardiac function in primates using real-time three-dimensional echocardiography as applications to safety assessment. J Pharmacol Toxicol Methods. 2005;52(1):182–7.
14. Sleeper MM, et al. Echocardiographic reference ranges for sedated healthy cynomolgus monkeys (Macaca fascicularis). J Am Assoc Lab Anim Sci. 2008;47(1):22–5.
15. Tang HL, et al. Evaluation of the cardiovascular function of older adult Rhesus monkeys by ultrasonography. J Med Primatol. 2008;37(2):101–8.
16. Ueda Y, et al. Echocardiographic parameters of clinically normal Geriatric Rhesus Macaques (Macacamulatta). J Am Assoc Lab Anim Sci. 2017;56(4):361–8.
17. Ueda Y, et al. Echocardiographic reference intervals with allometric scaling of 823 clinically healthy rhesus macaques (Macaca mulatta). BMC Vet Res. 2020;16(1):348.
18. Colman RJ. Non-human primates as a model for aging. Biochim Biophys Acta Mol Basis Dis. 2018;1864(9 Pt A):2733–41.
19. Chiou KL, et al. Rhesus macaques as a tractable physiological model of human ageing. Philos Trans R Soc Lond B Biol Sci. 1811;2020(375):20190612.
20. Liu CT, Higbee GA. Determination of body surface area in the rhesus monkey. J Appl Physiol. 1976;40(1):101–4.
21. Lang RM, et al. Recommendations for cardiac chamber quantification by echocardiography in adults: an update from the American Society of Echocardiography and the European Association of Cardiovascular Imaging. J Am Soc Echocardiogr. 2015;28(1):1-39.e14.
22. Devereux RB, Reichek N. Echocardiographic determination of left ventricular mass in man. Anatomic validation of the method. Circulation. 1977;55(4):613–8.
23. Pepi M, et al. A new formula for echo-Doppler estimation of right ventricular systolic pressure. J Am Soc Echocardiogr. 1994;7(1):20–6.
24. Chima AM, Mahmoud MA, Narayanasamy S. What is the role of dexmedetomidine in modern anesthesia and critical care? Adv Anesth. 2022;40(1):111–30.
25. Osnabrugge RL, et al. Aortic stenosis in the elderly: disease prevalence and number of candidates for transcatheter aortic valve replacement: a meta-analysis and modeling study. J Am Coll Cardiol. 2013;62(11):1002–12.
26. Simmons HA. Age-associated pathology in Rhesus Macaques (Macaca mulatta). Vet Pathol. 2016;53(2):399–416.
27. Gerstenblith G, et al. Echocardiographic assessment of a normal adult aging population. Circulation. 1977;56(2):273–8.
28. Lang RM, et al. Recommendations for cardiac chamber quantification by echocardiography in adults: an update from the American Society of Echocardiography and the European Association of Cardiovascular Imaging. Eur Heart J Cardiovasc Imaging. 2015;16(3):233–70.
29. Nakayama S, et al. Echocardiographic evaluation of cardiac function in cynomolgus monkeys over a wide age range. Exp Anim. 2020;69(3):336–44.
30. Ueda Y, et al. Identifying cardiac diseases using cardiac biomarkers in Rhesus Macaques (Macaca mulatta). Comp Med. 2020;70(5):348–57.
31. Ponikowski P, et al. 2016 ESC Guidelines for the diagnosis and treatment of acute and chronic heart failure: The

Task Force for the diagnosis and treatment of acute and chronic heart failure of the European Society of Cardiology (ESC)Developed with the special contribution of the Heart Failure Association (HFA) of the ESC. Eur Heart J. 2016;37(27):2129–200.
32. Chagas J, et al. Anaesthetic and cardiorespiratory effects of ketamine plus dexmedetomidine for chemical restraint in black capuchin monkeys (Sapajus nigritus). N Z Vet J. 2018;66(2):79–84.
33. Gu H, et al. Left ventricular diastolic dysfunction in non-human primate model of dysmetabolism and diabetes. BMC Cardiovasc Disord. 2015;15:141.
34. Qian C, et al. Diastolic dysfunction in spontaneous type 2 diabetes rhesus monkeys: a study using echocardiography and magnetic resonance imaging. BMC Cardiovasc Disord. 2015;15:59.
35. Zhu T, et al. 2D/3D CMR tissue tracking versus CMR tagging in the assessment of spontaneous T2DM rhesus monkeys with isolated diastolic dysfunction. BMC Med Imaging. 2018;18(1):47.
36. Liang Y, et al. Abstract 24055: Naturally occurring hypertension is related to cardiac diastolic dysfunction in Rhesus Monkeys. Circulation. 2017;136(suppl_1):A24055–A24055.
37. Zhen N, et al. A diastolic dysfunction model in non-human primates with transverse aortic constriction. Exp Anim. 2021;70(4):498–507.
38. Mantero A, et al. Left ventricular diastolic parameters in 288 normal subjects from 20 to 80 years old. Eur Heart J. 1995;16(1):94–105.